TRANSPORT PROBLEMS 2022 Volume 17 Issue 4
PROBLEMY TRANSPORTU DOI: 10.20858/tp.2022.17.4.03

Keywords: floating ring bearing; oil viscosity; radial slide bearing

Aleksander MAZURKOW[1]*, Wojciech HOMIK[2], Łukasz KONIECZNY[3]

STUDY OF RADIAL SLIDE BEARINGS WITH A FLOATING RING CONSIDERING THE PHYSICAL PROPERTIES OF OIL

Summary. Radial slide bearings are typically used in turbochargers (among other applications), owing to their simple design and advantages, such as good heat dissipation from the working zone, high stability of operation and low resistance to motion. The current research is both experimental and theoretical. In a state of static equilibrium, the operation of a bearing can be described using a system of five coupled differential equations. The bearing's operating parameters are related to the type of oil used. Two types of oil, VG46 and VG68, were used for testing. In accordance with the applicable standard, the tolerance of kinematic viscosity of oils is ±10%. The results imply a significant influence of the oil class and viscosity tolerance on the resistance to motion caused by internal friction forces in the oil. In conclusion, it seems advisable that the calculation procedures currently in use should include the slide bearing design optimisation by taking the resistance to motion in the bearing into account.

1. INTRODUCTION

Machine operation safety is a key issue in transport, including the branches of air, rail, road and industrial transport. Using slide bearings in these machines determines the possibility of safe operation in extreme conditions, such as under increased operating temperatures. The thermal properties and the resulting resistance of the bearings to high temperatures are of great importance in preventing serious incidents, including fires. Currently, materials such as stainless steel and bronze are widely used, but ceramics are also becoming popular owing to their ability to transfer sudden accelerations and high speeds. There is a noticeable trend of replacing metal bearings with self-lubricating plastic bearings in transport, especially in aviation applications, due to their lightness; durability; low price and resistance to dirt, dust and chemicals.

Plain bearings are commonly used in reciprocating and rotating machines. An example is internal combustion engines used in propulsion systems that use plain bearings as the main bearings to hold the crankshaft in the engine crankcase or connect the pin to the piston and connecting rod. Slide bearings with floating rings are used in internal combustion engines and turbochargers (e.g. those manufactured by Volkswagen Group, MAN Truck & Bus and Napier Turbochargers), among other applications.

Compared to classic designs, the bearings in question are characterised by low resistance to motion, good heat dissipation and high operating stability.

This bearing type comprises the following elements (Fig. 1): a journal (2), a fixed bearing bush (1) and a floating ring (3) loosely inserted between the journal and the fixed bearing bush. The floating ring divides the oil film generated during the bearing operation into the outer and inner oil film. Oil is

[1] Rzeszów University of Technology, Faculty of Mechanical Engineering and Aeronautics; al. Powstańców Warszawy 8, 35-959 Rzeszów, Poland; e-mail: almaz@prz.edu.pl; orcid.org/0000-0003-1719-991X
[2] Rzeszów University of Technology, Faculty of Mechanical Engineering and Aeronautics; al. Powstańców Warszawy 8, 35-959 Rzeszów, Poland; e-mail: whomik@prz.edu.pl; orcid.org/0000-0001-7843-7761
[3] Silesian University of Technology, Faculty of Transport and Aviation Engineering; Krasińskiego 8, 40-019 Katowice, Poland; e-mail: lukasz.konieczny@polsl.pl; orcid.org/0000-0002-9501-7651
* Corresponding author. E-mail: almaz@prz.edu.pl

supplied by an external source and it is delivered to both the floating ring and the fixed bearing bush through circumferential lubricant grooves (4). It flows to the fixed bearing bush via supply holes (5) and to the floating ring via another set of holes (6). The arrows show the oil flow direction inside the bearing (7).

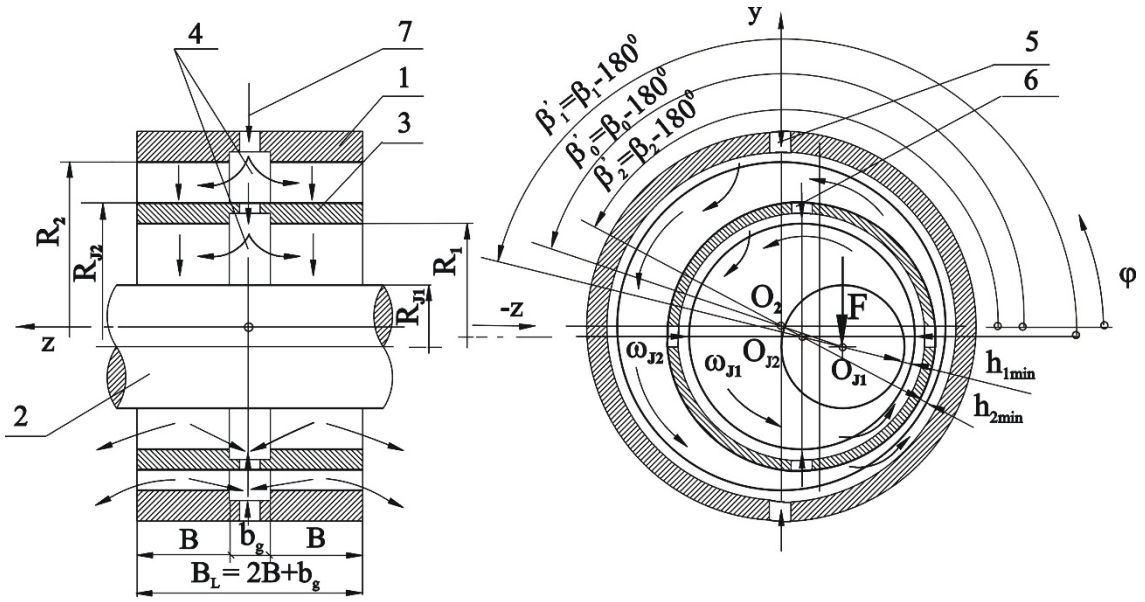

Fig. 1. Geometry and oil flow direction in a radial slide bearing with a floating ring: 1- fixed bearing bush, 2 – journal, 3 - floating ring, 4 - circumferential lubricant grooves, 5 and 6 - supply holes

Contemporary research concerns the modelling of oil and heat flow in a bearing for the positions of static [1÷6] and dynamic equilibria [7÷11].

Buluschek R. [12] presented the results of theoretical and experimental research on stationary operating conditions of an axially supplied floating ring bearing. For the theoretical research, an isothermal bearing model was adopted. The temperature of the oil films was determined by heat balances. The oil flow was assumed to be bidirectional (i.e. circumferential and axial in direction). The experimental research showed that the motion of the floating ring was unstable. Such instabilities were documented, and an attempt was made to describe the causes of this phenomenon by comparing the operation of the bearing to that of a viscous coupling.

The paper by D. M. Clarke, C. Fall, G. N. Hayden and T. S. Wilkinson [13] comments upon their theoretical research on a slide bearing with a floating ring for a constant load case and an adiabatic model. The model was built based on the assumption that the ring surfaces were perfectly cylindrical, while the pressure distribution equations were solved using the Gümbel boundary conditions. The heat from the bearing was dissipated by the flowing oil and radially through the surface of the floating ring and the journal. These assumptions made it possible to lower the order of the differential equation of temperature distribution.

In the theoretical part of a paper dedicated to a rotor featuring symmetrically arranged bearings, B. Domes [14] studied the effect of non-linear forces acting on the oil film on the formation of self-excited vibrations using an isothermal bearing model in the calculations. He determined the ranges of stable operation areas. The research was conducted for both a rotating and a non-rotating floating ring. The equilibrium of the position of the floating ring was considered against the condition of equilibrium of the moments of friction on the inner and outer surfaces of the floating ring, as well as in the frontal plane. The research concerned an axial bearing, and the experimental part included tests of high-speed rotors. The rotational speed of the rotating floating ring, as well as the amplitude and frequency of vibrations, were measured for the variable speed of the rotor and for variable unbalance.

Krause R. [15] conducted both theoretical and experimental studies. In the theoretical part, he built a substitute model of a bearing, while in the experimental section, for the assumed load and shaft rotational speed, he calculated the coefficients of stiffness and damping of the oil film and determined

the static positions of equilibrium of the journal and the floating ring. Additionally, for a rotor loaded by variable unbalance, he measured the rotational speed of the floating ring. The experiments were carried out for rotational speeds of the journal ranging from 700 to 5,000 rpm, with the static bearing load ranging from 500 to 25,000 N and the dynamic bearing load ranging from 50 to 3,000 N. The author also noticed that the oil film temperature depended on the bearing's dynamic properties. The coefficients of stiffness and damping were compared with the results of the theoretical work by Fink and Someya.

H. Allmaier, C. Priestner, F. M. Reich, H. H. Priebsch and F. Novotny-Farkas [16] presented a thermo-elastohydrodynamic (TEHD) model of a radial bearing that takes friction losses into account. The results were verified experimentally. Comparative studies of the EHD and THD models show that considering local temperatures results in relatively small corrections of the properties examined. Moreover, the TEHD results formed the basis for developing a method to establish the effective temperature of the EHD oil film. Yanyan Zhang, Lihua Yang, Zhi Li and Lie Yu [17] elaborated on a method envisaged for the static performance testing of hydrodynamically lubricated thrust slide bearings using harmonic functions. The authors defined a dimensionless function of the oil film thickness. Then, dimensionless pressure distributions and their corresponding hydrodynamic buoyancy forces were determined. Thus, the obtained results demonstrate the relationships between the thickness of the lube oil film, the pressure field and the hydrodynamic buoyancy force.

D. E. Sander, H. Allmaier, H. H. Priebsch, M. Witt and A. Skiadas [18] discussed researched bearings operating in a mixed and hydrodynamic lubrication regime. They experimentally identified the properties of the oil film under high pressure and high shear rate. The results were presented as Stribeck curves. The authors also found that temperature exerted a limited effect on the properties of the elastohydrodynamic oil film.

Yajing Li, Feng Liang, Yu Zhou, Shuiting Ding, Farong Du, Ming Zhou, Jinguang Bi and Yi Cai [19] conducted theoretical and experimental research on high-speed rotor systems. They analysed the impact of oil temperature and viscosity on the operating parameters of a test bearing. Theoretical research was conducted for a three-dimensional heat and oil flow in the bearing. The authors concluded that, compared to a two-dimensional model, the three-dimensional flow model reflected real-life operating conditions much more accurately.

The operating parameters of a bearing can be established through theoretical [20÷23] or experimental research [24÷29]. In theoretical research, three types of models are used: isothermal, adiabatic and diathermic. In the isothermal model, the oil film temperature is constant. In the adiabatic model, the heat generated is removed from the working zone by the flowing oil. Meanwhile, in the diathermic model, heat is dissipated by the flowing oil and the housing components. This paper presents the relevant research results obtained for the adiabatic model.

The methods used when designing slide bearings have been based on verified theoretical models whose outputs include bearing characteristics established under static and dynamic equilibria. These characteristics are necessary to analyse the results of calculations performed using the mathematical model. The limitations assumed in calculation methods are as follows: permissible pressure (p_{lim}), maximum permissible temperature (T_{lim}) and the minimum permissible height of a lubrication gap (h_{lim}). These values are determined for laminar flows. This paper proposes that the methods in question should be supplemented with calculations of the bearing's resistance to motion. For slide bearings with a floating ring, this is the frictional moment on the surface of the fixed bearing bush (M_{t4}). Following the applicable standards, oils are characterised by standard viscosity with a tolerance of $\nu = \pm 10\%$ [mm^2/s]. An analysis of the available literature has revealed that no research results show how oil viscosity tolerance affects resistance to motion.

2. MATERIALS AND METHODS

2.1. Analysis of forces and moments of friction in a bearing

In the state of thermohydrodynamic equilibrium, when applied to the bearing journal, external load F, constant in terms of direction and magnitude, is balanced by the hydrodynamic capacity of the inner

bearing (F_{L1}) and of the outer bearing (F_{L2}) (Fig. 2). The centres of the journal (O_{J1}) and the floating ring (O_{J2}) are displaced eccentrically with respect to each other and against the centre of the fixed bearing bush (O_2). The journal centre displacement values are described by eccentricities e_1, e_2 and e_0. The distances between the load effect line and the oil film reaction line are determined by displacements e'_1 and e'_2.

The moments of friction designated as $M_2(O_{J2})$ and $M_3(O_{J2})$, observed on the outer and inner surfaces of the floating ring, are equal. $M_1(O_{J1})$ and $M_4(O_{J2})$ are the moments of friction on the surface of the journal and the fixed bearing bush, respectively. Additional information about the geometry of the lubricating films has been provided in previous work [30].

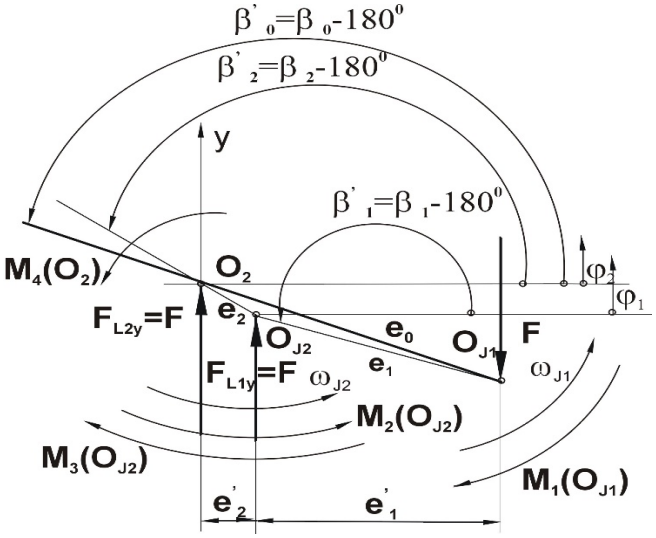

Fig. 2. Forces and moments of friction in a radial slide bearing with a floating ring

2.2. Theoretical model of a slide bearing with a floating ring

The theoretical model is based on specific assumptions regarding the oil and heat flow in the bearing, the structure of the bearing elements and the lubricant [30]. These assumptions include the following:
- bearing elements are non-deformable and perfectly smooth cylindrical surfaces with parallel axes;
- oil is an incompressible Newtonian fluid of constant conductivity and variable specific heat capacity, viscosity and density, which depend solely on temperature;
- flow is laminar;
- heat flow and oil flow coincide and there is no heat exchange between the oil film and sliding surfaces;
- the heat conduction capacity of oil is taken into account;
- the oil temperature in the radial direction is constant;
- the temperature in the bearing's supply groove is constant (T_z = const.);
- the values of oil temperature in the circumferential oil grooves are constant and are determined by the heat balance. These temperatures vary for the inner and the outer bearing, amounting to T_{ol1} = const and T_{ol2} = const, respectively;
- the pressure generated in the oil film may be greater than or equal to zero;
- the oil pressure in the supply grooves and the ambient pressure are constant.

- **Equation of pressure distribution in lubrication gaps (i = 1, 2):**

The equation describing the distribution of pressure in the oil film was obtained by transforming the Stokes-Navier equation and the equation of flow continuity:

$$\frac{\partial}{\partial x_i}\left(\frac{h_i^3}{\eta}\cdot\frac{\partial p_i}{\partial x_i}\right)+\frac{\partial}{\partial z}\left(\frac{h_i^3}{\eta}\cdot\frac{\partial p_i}{\partial z}\right)=6\cdot\left(\omega_i\cdot R_i+\omega_{i+1}\cdot R_{i+1}\right)\cdot\frac{\partial h_i}{\partial x_i} \tag{1}$$

Meanwhile, if $\begin{cases} i=1 & \omega_i\cdot R_i=\omega_{J1}\cdot R_{J1}, \\ i=2 & \omega_i\cdot R_i=\omega_{J2}\cdot R_{J2}, \omega_{i+1}\cdot R_{i+1}=0, \end{cases}$

- **Equation of the shape of lubrication gaps (i = 1, 2):**

For testing purposes, it was assumed that the journal, the floating ring and the fixed bearing bush were cylindrically shaped. For the φ angle describing the angular coordinate and the βangle describing the position of the centre line (Fig. 2), the equation of the shape of lubrication gaps in the dimensional form is given by

$$h_i = C_{Ri} \cdot \left[1 + \varepsilon_i \cdot cos\left(\varphi_i - \beta_i\right)\right] \tag{2}$$

- **Equation of temperature distribution in lubrication gaps (i = 1, 2):**

For the assumed adiabatic model, the equation of temperature distribution was derived from the energy equilibrium equation. Simplifications concerning the flow and transfer of heat, as well as the lubricant properties, were assumed [30]. The temperature distribution equation assumes the following dimensional form:

$$\rho \cdot c_p \left[\upsilon_{xi} \frac{\partial T_i}{\partial x_i} + \upsilon_{zi} \frac{\partial T_i}{\partial z} \right] = \lambda \cdot \Delta T_i + \eta \left[\left[\frac{\partial \upsilon_{xi}}{\partial y_i} \right]^2 + \left[\frac{\partial \upsilon_{zi}}{\partial y_i} \right]^2 \right], \tag{3}$$

Based on Equation (3), the components of the flow velocity along the *x* and *z* axes are described by the following relationships:

$$\upsilon_{xi} = \frac{1}{2\eta} \frac{\partial p_i}{\partial x_i} y_i \left(y_i - h_i\right) + \frac{\omega_{i+1} \cdot R_{i+1}}{h_i} \left(h_i + y_i\right) + \frac{\omega_i \cdot R_i}{h_i} y_i, \; \upsilon_{zi} = \frac{1}{2\eta} \frac{\partial p_i}{\partial z} y_i \left(y_i - h_i\right),$$

- **Equations of equilibrium of forces and moments of friction:**

In the state of thermohydrodynamic equilibrium (Fig. 2), the centres of the journal (O_{J1}) and the floating ring (O_{J2}) are eccentrically displaced against the centre of the fixed bearing bush (O_2). When this is the case, the conditions of equilibrium are described by the equations of equilibrium of oil forces in both oil films (F_L), balanced by the load (F) and the moments of friction on the inner and outer surfaces of the floating ring. The conditions are described by the following system of equilibrium equations:

$$\begin{cases} F_{L1x} = F_{L2x} = 0 \\ F_{Ly1} = F_{Ly2} = F \\ M_2(O_{J2}) = M_3(O_{J2}) \end{cases} \tag{4}$$

The condition of equilibrium of the moments of friction takes the following form:

$$\begin{aligned} &\frac{-R_{J2}}{F_{Ly2}} \int_0^{2\pi} \left(\frac{1}{2} \cdot \psi_2 \cdot B \cdot h_2 \cdot \frac{\partial p_2}{\partial \varphi_2} + \frac{B \cdot \omega_2 \cdot \eta}{\psi_2 \cdot h_2} \right) d\varphi_2 = \\ &= \frac{R_{J1}}{R_{J2}} \cdot \frac{-R_{J1}}{F_{Ly1}} \int_0^{2\pi} \left(\frac{1}{2} \cdot \psi_1 \cdot B \cdot h_i \cdot \frac{\partial p_1}{\partial \varphi_1} + \frac{B \cdot \omega_1 \cdot \eta}{\psi_1 \cdot h_1} \left(1 - \Omega \frac{R_1}{R_{J1}} \right) \right) d\varphi_1 - \psi_1 \varepsilon_1 \cdot \sin \beta_1. \end{aligned} \tag{5}$$

Additional information on the derivation of Equations (2-5) has been provided in previous papers [30].

2.3. Equations of the state of lubricant

The local values of viscosity, density, specific heat capacity and thermal conductivity of oil are needed to determine the distribution of pressure and temperature in the lubrication film. The classification according to standard [31, 32] was used in order to describe the properties of oil. In accordance with the classification the acceptable tolerance level for the kinematic viscosity of oil is $\nu = \pm 10\%$.

The dynamic viscosity of oil is described by the following exponential function [12, 30]:

$$\eta = \eta_0 \cdot e^{a_\eta (T - T_0) + b_\eta (T - T_0)^2}, \tag{6}$$

where a_η, b_η is the factor determining the effect of temperature on dynamic viscosity.

The studies were performed for two VG_{46} and VG_{68} class oils. The functions of oil viscosity (taking the tolerance of $\upsilon = \pm 10\%$ into account) are represented by the following equations:

$$\eta(T)\big|_{VG_{68\,min}} = 0{,}1786 \cdot e^{-0{,}648 a_\eta (T-T_0)+0{,}00030159(T-T_0)^2},$$
$$\eta(T)\big|_{VG_{68\,max}} = 0{,}2268 \cdot e^{-0{,}671\cdot(T-T_0)+0{,}00031205\cdot(T-T_0)^2},$$
$$\eta(T)\big|_{VG_{46\,min}} = 0{,}1115 \cdot e^{-0{,}604\cdot(T-T_0)+0{,}00028177\cdot(T-T_0)^2},$$
$$\eta(T)\big|_{VG_{46\,max}} = 0{,}142 \cdot e^{--0{,}628\cdot(T-T_0)+0{,}00029269(T-T_0)^2}, \tag{7}$$

The functions of the density, specific heat capacity and thermal conductivity of the oil were assumed to be constant per DIN 31652:

$$\rho(T) = const, \tag{8}$$
$$c_p(T) = const, \tag{9}$$
$$\lambda = const \tag{10}$$

2.4. Boundary conditions for the field of pressure and temperature

When determining the boundary conditions for the field of pressure and temperature [33], it was assumed that the oil grooves in the inner and outer bearings were filled with oil. Given these assumptions, the boundary conditions of the pressure field are as follows (Fig. 3):
- at the border between the supply groove and the bearing bush: $p(\varphi_i, -B/2) = p_z$,
- at the boundary between the bearing bush and its surroundings: $p(\varphi_i, B/2) = 0$,
- at the boundary between the working and non-working zones: $\frac{\partial p_i}{\partial \varphi_i} = 0$,
- on the surface of both bearing bushes: $p_i(<0.2\pi>, z) \geq 0$,

Three zones were defined to describe the boundary conditions of the temperature field (Fig. 4):
- the zone containing the boundary between the bearing bush and the supply groove, in which the temperature is constant,
- the zone containing the boundary between the bearing bush and the supply groove or between the bearing bush and its surroundings, in which the temperature varies,
- the zone on the surface of the bearing bush, in which pressure equals zero, which contains the boundary where oil is fading.

Fig. 4 presents the conditions at the boundaries of the bearing bush assumed when solving the equations of the temperature field. In [30], the author describes how to derive dependencies describing the temperature gradients (Fig. 4) at the boundaries between the working and the non-working zone, $\frac{\partial T_i}{\partial x} = \beta_x$, between the working zone and the supply groove and between the working zone and the bearing bush surroundings: $\frac{\partial T_i}{\partial z} = \beta_z$. The functions are given by the following formulas:

$$\frac{\partial T_i}{\partial x} = \beta_x = \frac{\eta(\upsilon_{xi}^{**} + \upsilon_z^{**})\cdot \upsilon_{xi}^{*}}{\rho \cdot c_p((\upsilon_z^{*})^2 + (\upsilon_{xi}^{*})^2)} \qquad \frac{\partial T_i}{\partial z} = \beta_z = \frac{\eta(\upsilon_{xi}^{**} + \upsilon_z^{**})\cdot \upsilon_{z}^{*}}{\rho \cdot c_p((\upsilon_z^{*})^2 + (\upsilon_{xi}^{*})^2)} \tag{11}$$

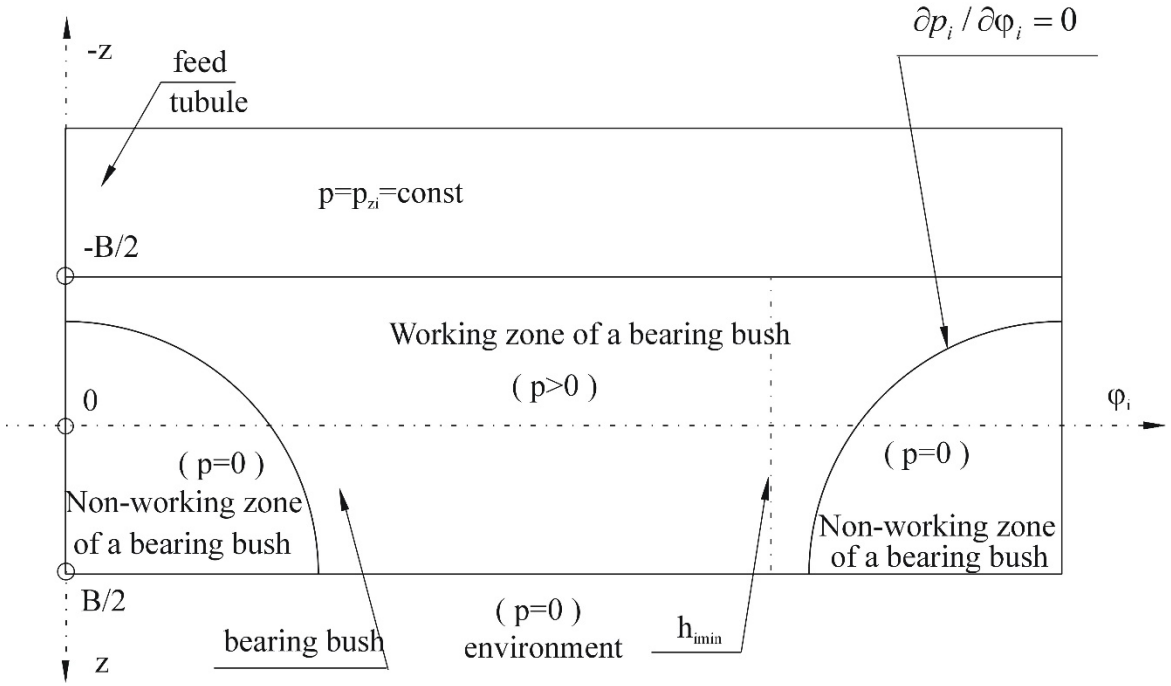

Fig. 3. Boundary conditions of the pressure field

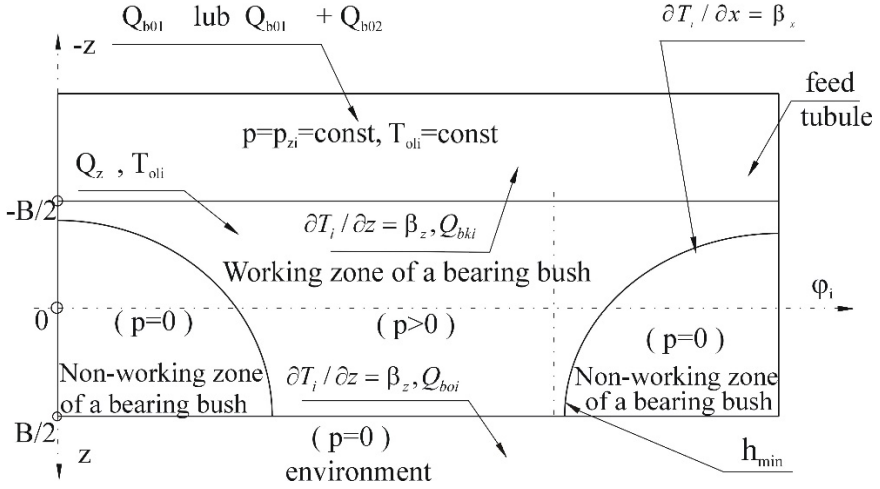

Fig. 4. Boundary conditions of the temperature field

where

$$\upsilon_{xi}^{*} = \int_0^h \upsilon_{xi} \cdot dy, \quad \upsilon_{zi}^{*} = \int_0^h \upsilon_{zi} \cdot dy \tag{12}$$

$$\upsilon_{xi}^{**} = \int_0^h \left(\frac{\partial \upsilon_{xi}}{\partial y_i} \right)^2 \cdot dy, \qquad \upsilon_{zi}^{**} = \int_0^h \left(\frac{\partial \upsilon_{zi}}{\partial y_i} \right)^2 \cdot dy \cdot$$

2.5. The algorithm and method used to solve the system of equations of the mathematical bearing model

The mid-width of the fixed bearing bush and the floating ring (Fig. 1) contain circumferential grooves that divide them into two halves. In the case under consideration, a reference system was used; the angular coordinate (φ) was assumed to be in the middle of the width of one of the halves.

A coupled system of five differential equations for the state of static equilibrium can be solved by assuming that the position of one of the two journals or the load represents a pre-set value. In the first case, one should look for a hydrodynamic force which balances the load, while in the second case, one should look for a position in which the hydrodynamic force balances the load. The system of equations was solved numerically, assuming the position of the floating ring against the fixed bearing bush as a pre-set value. The differential equations were solved using the finite difference method. As per standard [32], the assumed accuracies of the calculated values were obtained iteratively. The solution of the mathematical model equations can be presented as the following algorithm:

Stage 1. Pre-set parameters:

- temperature and pressure of oil in the bearing: $T_{zas}[^0C]$, $p_{zas}[N/m^2]$,
- angular velocity of the floating ring: ω_2[rad/s],
- physical properties of oil: $\eta(T)$ [Pa·s], $\rho(T)$ [kg/m^3], λ[W/(m·^{o}C)], $c_p(T)$ [J/(kg·^{o}C)],
- position of the centre of the floating ring: ε_2,
- geometry of the bearing: R_{J1}, R_1, R_{J2}, R_2, B [m].

Stage 2. Operating parameters of the bearing determined for the isothermal model:

- based on the equations of equilibrium of forces and moments: angular velocity of the journal – ω_1, relative eccentricity of the inner bearing – ε_1, resultant relative eccentricity – ε_0, angles defining the location of centre lines – β_1, β_2, β_0, the bearing's hydrodynamic force of oil – F,
- pressure distribution in the oil films $p_1(\varphi_1, z)$, $p_2(\varphi_2, z)$.

At this stage, the dynamic viscosity in the working zone of the bearing bush was assumed to be constant η = const.

Stage 3. Operating parameters of the bearing determined for the adiabatic model:

- temperature distribution in the oil films $T_1(\varphi_1, z)$, $T_2(\varphi_2, z)$.
- the hydrodynamic force of the oil film F_{L1}, F_{L2},
- moment of friction on the surface of fixed bearing bush M_{t4},
- the angular velocity of journal ω_1.

Similarly to stage 2, the equations of the temperature distribution in both lubricant films were assumed to be dimensionless for calculation purposes. An exact algorithm of the solution, the solution method and the confirmation of the theoretical model's compliance with the bench test results have been provided in other papers [12, 29, 30]. Fig. 5 provides a flowchart illustrating the method used to solve the mathematical model in question.

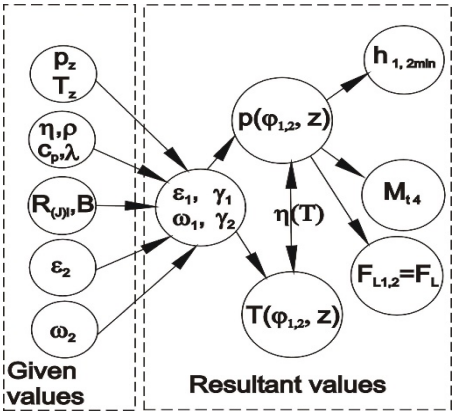

Fig. 5. Flowchart of the method assumed for solving the mathematical model

3. RESULTS

The effect of oil viscosity tolerance on the operating parameters of the bearing, such as the hydrodynamic force of oil film (F_{L1}, F_{L2}), the moment of friction on the bush surface (M_{t4}), the angular velocity of the journal (ω_1) and the maximum temperatures in the oil films (T_{1max}, T_{2max}), was tested for the pre-set values listed in Table 1.

Table 1

Pre-set values

Parameter value
1. Journal diameter, inner and outer bearing: D_{J1} = 31.636; D_{J2} = 37.986 mm
2. Outer diameter of the inner and outer bearing: D_1 = 31.765; D_2 = 38.115 mm
3. Bearing width: B = 22.22 mm
4. Relative eccentricity: ε = <0.2-0.9>
5. Rotational speed of the floating ring: ω_{J2} = 1,000 1/s, n_{J1} = 9,549.3 rpm
6. Oil class VG46 and VG68, viscosity tolerance: $\nu = \pm 10\%$
7. Oil density: ρ_0 = 900 [kg/m^3]
8. Specific heat capacity: c_{p0} = 2,000 [J/kg·^{0}C]
9. Ambient temperature and temperature of oil supplied to the bearing: T_0 = 20 °C, T_z = 50 °C
10. Pressure of oil supplied to the bearing: p_z = 0.1 MPa

The pre-set values were used in the calculations, and the results are provided in the graphs depicted in Fig. 6, as well as in Table 2.

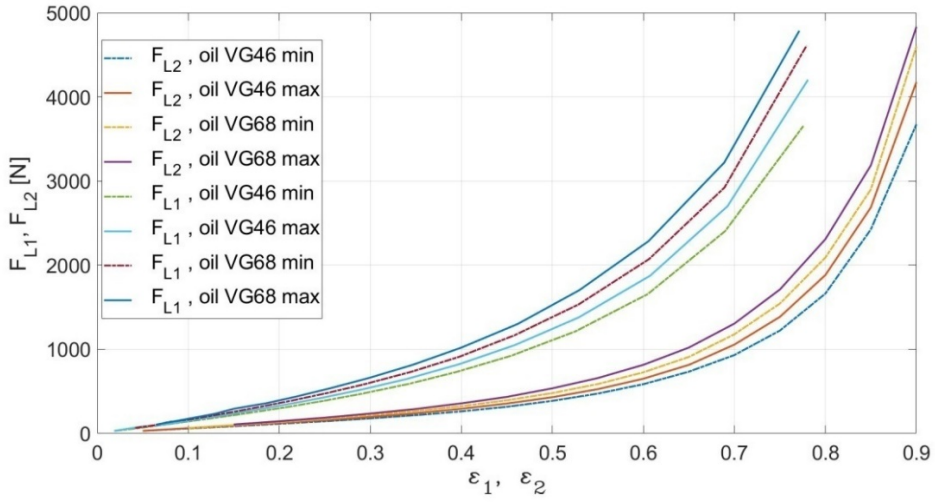

a)

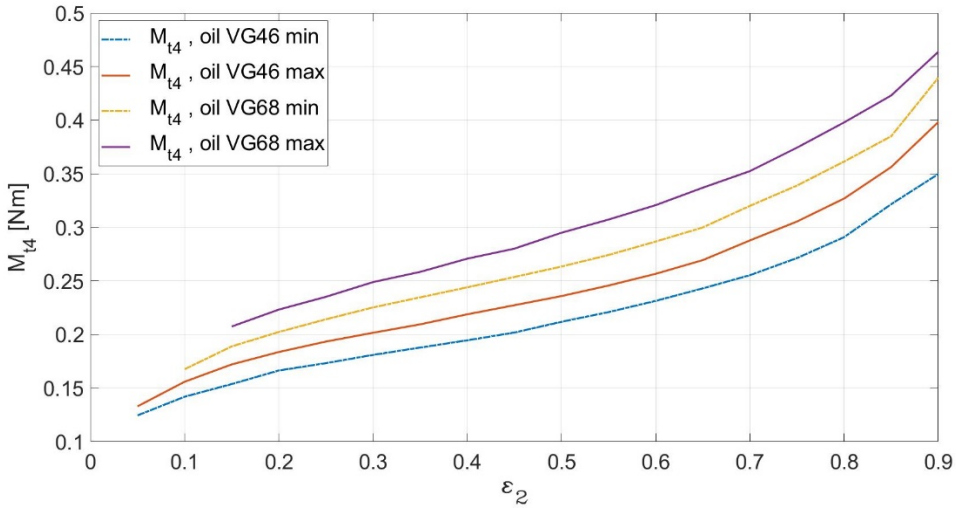

b)

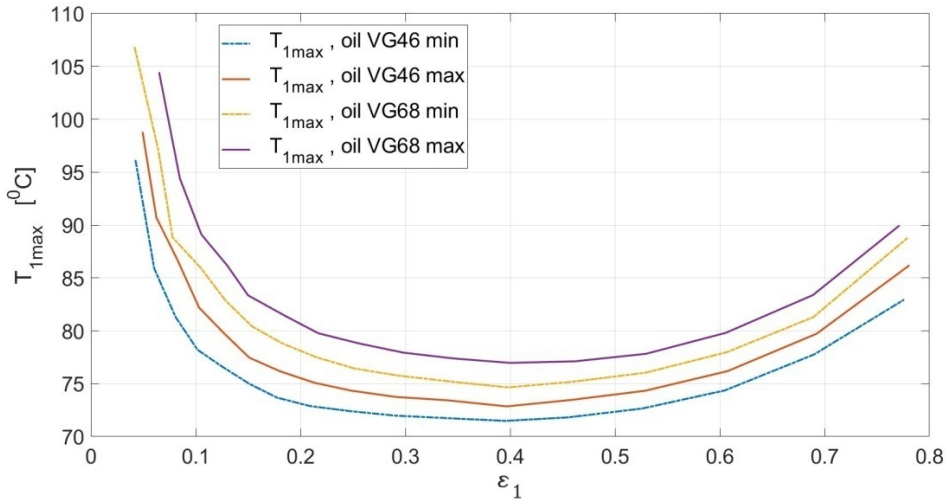

c)

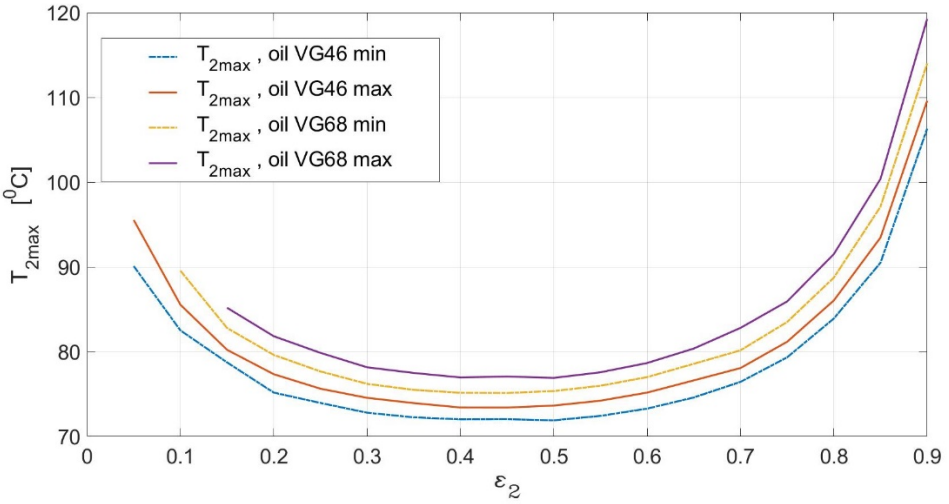

d)

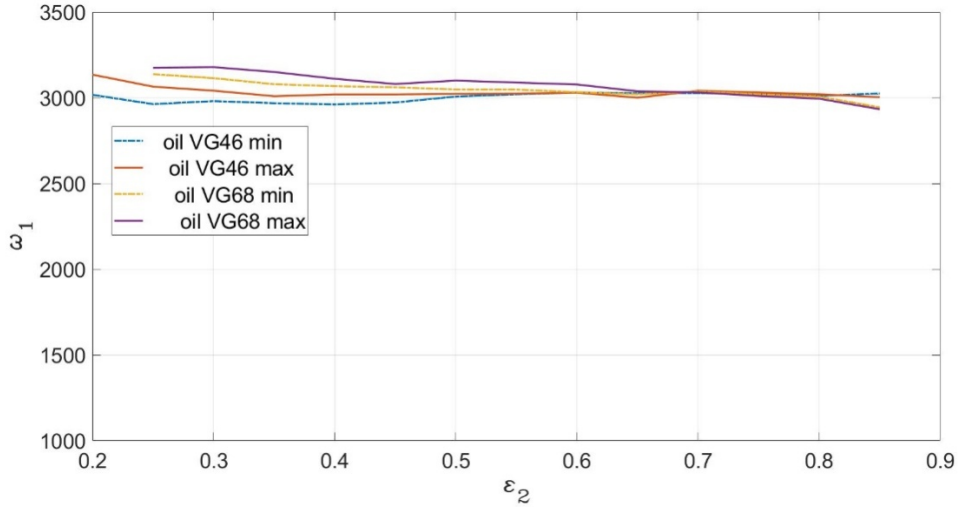

e)

Fig. 6. Effect of oil viscosity tolerance on the bearing's operating parameters:
a) $F_L = F_L(\varepsilon_1, \varepsilon_2)$, b) $M_{t4} = M_{t4}(\varepsilon_2)$, c) $T_{1max} = T_{1max}(\varepsilon_1)$, d) $T_{2max} = T_{2max}(\varepsilon_2)$, e) $\omega_1 = \omega_1(\varepsilon_2)$

Table 2

Operating parameters of the bearing

Operating parameter	**Calculation results**					
F_L [N]	500	1,500	2,500	1,500	1,500	2,500
	Oil type					
	VG_{68max}			**VG_{46max}**		
ε_2 [-]	0.469	0.702	0.801	0.539	0.762	0.838
ε_1 [–]	0.241	0.493	0.624	0.276	0.548	0.672
T_{2max}[°C]	77	84	94	73.9	82.5	91.3
T_{1max}[°C]	79.1	77.4	80.7	74	74.9	79
M_{t4} [Nm]	0.285	0.36	0.404	0.243	0.307	0.347
p_{2max}[MPa]	1.25	5.11	10.28	1.39	4.72	10.28
p_{1max} [MPa]	1.31	4.72	9.17	1.33	5.11	9.78
h_{2min}[μm]	34.4	18.4	12	30	15.6	10.1
h_{1min} [μm]	49.3	32.7	24.7	46.7	28.7	20.7

Oil type						
	VG_{68min}			**VG_{46min}**		
ε2 [-]	0.503	0.741	0.828	0.569	0.785	0.854
ε1 [-]	0.266	0.521	0.648	0.301	0.579	0.699
T_{2max}[°C]	75.5	82.5	93.5	72.6	82.4	90.4
T_{1max}[°C]	76.1	76.7	79.7	72	75.5	80
M_{t4}[Nm]	0.265	0.335	0.3778	0.227	0.283	0.327
p_{2max}[MPa]	1.39	5.28	10.56	1.39	5.97	10.28
p_{1max} [MPa]	1.39	5	9.44	1.36	5.33	9.78
h_{2min}[μm]	31.3	16.7	10.7	27.7	13.8	9.2
h_{1min}[μm]	47.3	31	22.7	45.2	27.7	19.3

The values of the moments of friction on the fixed bearing bush, considering the oil tolerance, are as follows:

$$\delta_{Mt4}^{VG68max/min} = \frac{M_{t4}(VG_{68max}) - M_{t4}(VG_{68min})}{Mt4(VG_{68min})} = \frac{0,36 - 0,335}{0,335} \cdot 100 = 7,5\%$$

$$\delta_{Mt4}^{VG46miax/min} = \frac{M_{t4}(VG_{46max}) - M_{t4}(VG_{46min})}{M_{t4}(VG_{46min})} = \frac{0,307 - 0,283}{0,283} \cdot 100 = 8,5\% \quad (13)$$

$$\delta_{Mt4}^{VG68min/VG46min} = \frac{M_{t4}(VG_{68min}) - M_{t4}(VG_{46max})}{M_{t4}(VG_{46max})} = \frac{0,335 - 0,307}{0,307} \cdot 100 = 9,1\%$$

$$\delta_{Mt4}^{VG68max/VG46min} = \frac{M_{t4}(VG_{68max}) - M_{t4}(VG_{46min})}{M_{t4}(VG_{46min})} = \frac{0,36 - 0,283}{0,283} \cdot 100 = 27,2\%$$

4. CONCLUSIONS

The mathematical model equations were solved for a given position of the floating ring against the fixed bearing bush. The bearing's static characteristics were established in order to determine the properties of the slide bearing featuring a floating ring.

An analysis of the operating parameters of the bearing (provided in Table 2) implies that the maximum values of pressure, temperature (p_{1max}, p_{2max}, T_{1max}, T_{2max}), the moment of friction on the surface of the fixed bearing bush (M_{t4}) increase as the bearing load ($F_{L1} = F_{L2} = F_L$) increases. At the same time, the minimum heights of lubrication gaps (h_{1min}, h_{2min}) decrease.

Furthermore, as the relative eccentricity rises to $\varepsilon_{1,2} \geq 0.5$, the oil film temperatures (T_{1max}, T_{2max}) decrease. A further increase to $\varepsilon_{1,2} > 0.5$ causes oil film temperatures to rise.

An additional analysis of the function graphs provided in Fig. 6 and the calculation results contained in Table 2 reveals that increasing eccentricity ε_2 results in an increase in the resistance to motion (M_{t4}). The values of p_{1max}, p_{2max}, T_{1max}, T_{2max}, h_{1min} and h_{2min} determine the proper operation of the bearing.

VG_{46} and VG_{68} oils represent the recommended and consecutive oil classes. The permissible tolerance of the kinematic viscosity ν of oil is ±10%. An analysis of the relationships given by the corresponding Equations (12) shows that the VG viscosity class and viscosity tolerance (ν) significantly affect the resistance to motion in the bearing (M_{t4}). The relative increases in the moment of friction for oil classes VG_{46} and VG_{68} were $\delta_{Mt4}^{VG_{46\,max/\,min}} = 8{,}5\%$, $\delta_{Mt4}^{VG_{68\,max/\,min}} = 7{,}5\%$, respectively. The relative increase in the moment of friction for VG_{46min} and VG_{48max} was $\delta_{Mt4}^{VG_{68\,min}/VG_{46\,min}} = 9{,}1\%$, while the relative increase for VG_{68max} and VG_{46min} was $\delta_{Mt4}^{VG_{68\,max}/VG_{46\,min}} = 27{,}2\%$.

The applicable standards and the available publications [12, 30, 32] presenting the methods used to calculate various types of bearings fail to consider the moment of friction as a criterion for optimising the operating parameters of a bearing. In light of the above analyses, we recommend including the aspect of the slide bearing design optimisation in the procedures applied in the present study while considering the resistance to motion in a bearing.

Abbreviations

B – ring width [m], C_R – radial clearance [m], D – diameter [m], h – oil film height [m], F – load [N], F_T – friction force [N], M_t – moment of friction [N·m]; n_J – rotational speed of journal [rpm], p – pressure in oil film [N/m^2], Q_{bk} – oil stream flowing from working zone to feed tubule [m^3/s], Q_{b0} – oil stream flowing from working zone to environment [m^3/s], R – radius [m]; T– temperature [^{o}C], x = φ·R – Cartesian coordinate [m], y – Cartesian coordinate [m], ω_J – angular velocity of journal [rad/s],
Indexes: J – journal; a rotor journal for the inner oil film or a floating ring for the outer oil film, i = 1– inner oil film, i = 2– outer oil film, lim – limit value, max – maximum value, min – minimum value.

References

1. Nikolic, N. & Antonic, Z. & Doric, J. & Ruzic, D. & Galambos, S. & Jocanovic, M. & Karanovic, V. An analytical method for the determination of the temperature distribution in short journal bearing oil film. *Symmetry.* 2020. Vol. 12. No. 4. Paper No. 539.
2. Ramos, D.J. & Daniel, G.B. A new concept of active hydrodynamic bearing for application in rotating systems. *Tribology International.* 2021. Vol. 153. Paper No. 106592.
3. Sadabadi, H. & Nezhad, A.S. Nanofluids for Performance Improvement of Heavy machinery. *Journal Bearings: A Simulation Study. Nanomaterials.* 2020. Vol. 10. Paper No. 2120.
4. Strzelecki, S. & Kuśmierz, L. & Poniewaz, G. Thermal deformation of pads in tilting 5-pad journal bearing. *Eksploatacja i Niezawodność – Maintenance and Reliability*. 2008. Vol. 38. No. 2. P. 12-16.

5. Wang, Y. & Fang, X. & Zhang, C. & Chen, X. & Lu, J. Lifetime prediction of self-lubricating spherical plain bearings based on physics-of-failure model and accelerated degradation test. *Eksploatacja i Niezawodność – Maintenance and Reliability.* 2016. Vol. 18. No. 4. P. 528-538.
6. Zhang, Y. & Yang, L. & Li, Z. & Yu, L. Research on static performance of hydrodynamically lubricated thrust slider bearing based on periodic harmonic. *Tribology International.* 2016. Vol. 95. P. 236-244.
7. Peixoto, T.F. & Cavalca, K.L. Thrust bearing coupling effects on the lateral dynamics of turbochargers. *Tribology International.* 2020. Vol. 145. Paper No. 106166.
8. Kim, S. & Palazzolo, A.B. Effects of thermohydrodynamic (THD) floating ring bearing model on rotordynamic bifurcation. *International Journal of Non-Linear Mechanics.* 2017. Vol. 95. P. 30-41.
9. Tian, L. & Wang, W.J. & Peng, Z.J. Dynamic behaviours of a full floating ring bearing supported turbocharger rotor with engine excitation. *Journal of Sound and Vibration.* 2011. Vol. 330. P. 4851-4874.
10. Chen, W.J. Rotordynamics and bearing design of turbochargers. *Mechanical Systems and Signal Processing.* 2012. Vol. 29. P. 77-89.
11. Wang, X. & Li, H. & Meng, G. Rotordynamic coefficients of a controllable magnetorheological fluid lubricated floating ring bearing. *Tribology International*. 2017. Vol. 114. P. 1-14.
12. Buluschek, B. *Das Schwimmbüchsenlager bei stationärem betrieb. PhD thesis.* Institut für Grundlagen der Maschinen Konstruktion. ETH Zürich. 1980. [In German: *Floating bush bearing under steady-state conditions. PhD thesis.* Institute of Fundamentals Mechanical Engineering. ETH Zürich. 1980].
13. Clarke, D.M. & Fall, C. & Hayden, G.N. & Wilkinson, T.S. A Steady – State Model of an Floating Ring Bearing, Including Thermal Effects. Trans. *ASME – Journal of Tribology.* 1992. Vol. 114.
14. Domes, B. *Amplituden der Unwucht – und Selbsterregen Schwingungen Hochtourigermit Rotierenden und nichtrotierenden Schwimmenden Büchsen. PhD thesis.* Universität Karlsruhe. 1980. [In German: *Amplitudes of imbalance and self-excited vibrations of high-speed rotating and non-rotating floating bushes. PhDthesis*. University of Karlsruhe. 1980].
15. Krause, R. *Experimentelle Untersuchungeines dynamisch beanspruchten Schwimmbüchsenlagers. PhD thesis.* Institutfür Grundlagen der Maschinen Konstruktion. ETH Zürich. 1987. [In German: *Experimental investigation of a dynamically stressed floating bush bearings. PhD thesis*. Institute of Fundamentals Mechanical Engineering. ETH Zürich. 1980].
16. Allmaier, H. & Priestner, C. & Reich, F.M. & Priebsch, H.H. & Novotny-Farkas, F. Predicting friction reliably and accurately in journal bearings—extending the EHD simulation model to TEHD. *Tribology International.* 2013. Vol. 58. P. 20-28.
17. Zhang, Y. & Yang, L. & Li, Z. & Yu, L. Research on static performance of hydrodynamically lubricated thrust slider bearing based on periodic harmonic Research on static performance of hydrodynamically lubricated thrust slider bearing based on periodic harmonic. *Tribology International*. 2016. Vol. 95. P. 236-244.
18. Sander, D.E. & Allmaier, H. & Priebsch, H.H. & Witt, M. & Skiadas, A. Simulation of journal bearing friction in severe mixed lubrication – Validation and effect of surface smoothing due to running. *Tribology International.* 2016. Vol. 96. P. 173-183.
19. Li, Y. & Liang, F. & Zhou, Y. & Ding, S. & Du, F. & Zhou, M. & Bi, J. & Cai, Y. Numerical and experimental investigation on thermohydrodynamic performance of turbocharger rotor-bearing system. *Applied Thermal Engineering.* 2017. Vol. 121. P. 27-38.
20. Adiletta, G. Stability Effects of Non-Circular Geometry in Floating Ring Bearings. *Lubricants*. 2020. Vol. 8. No 99.
21. Blaut, J. & Breńkacz, Ł. Applications of the Teager-Kaiser energy operator in diagnostics of a hydrodynamic bearing. *Eksploatacja i Niezawodność – Maintenance and Reliability*. 2020. Vol. 22. No. 4. P. 757-765.
22. Bernhauser, L. & Heinisch, M. & Schörgenhumer, M. & Nader, M. The Effect of Non-Circular Bearing Shapes in Hydrodynamic Journal Bearings on the Vibration Behavior of Turbocharger Structures. *Lubricants*. 2017. Vol. 5. No. 6.

23. Chasalevris, A. & Louis, J-C. Evaluation of Transient Response of Turbochargers and Turbines Using Database Method for the Nonlinear Forces of Journal Bearings. *Lubricants.* 2019. Vol. 7. No. 9. Paper No. 78.
24. Dyk, Š. & Smolík, L. & Rendl, J. Predictive capability of various linearization approaches for floating-ring bearings in nonlinear dynamics of turbochargers. *Mechanism and Machine Theory*. 2020. Vol. 149. No. 103843.
25. Feng, H. & Jiang, S. & Ji, A. Investigations of the static and dynamic characteristics of water-lubricated hydrodynamic journal bearing considering turbulent, thermohydrodynamic and misaligned effects. *Tribology International.* 2019. Vol. 130. P. 245-260.
26. Zhou, H-l. & Feng, G-q. & Luo, G-h. & Ai, Y-t. & Sun, D. The dynamic characteristics of a rotor supported on ball bearings with different floating ring squeeze film dampers. *Mechanism and Machine Theory*. 2014. Vol. 80. P. 200-213.
27. Jamalabadi, M.Y.A. & Alamian, R. & Yan, W-M. & Li, L.K.B. & Leveneur, S. & Shadloo, M.S. *Effects of Nanoparticle Enhanced Lubricant Films in Thermal Design of Plain Journal Bearings at High Reynolds Numbers*. *Symmetry.* 2019. Vol. 11. No. 11. Paper No. 1353.
28. Ryu, K. & Yi, H. Wire Mesh Dampers for Semi-Floating Ring Bearings in Automotive Turbochargers: Measurements of Structural Stiffness and Damping Parameters. *Energies.* 2018. Vol. 11. No. 4. Paper No. 812.
29. Budzik, G. & Mazurkow, A. Modelling and Testing of Dynamic Properties of C0-45 Turbochargers. *Scientific Journal of Silesian University of Technology. Series Transport.* 2017. Vol. 97. P. 17-25.
30. Mazurkow, A. *Teoria smarowania łożysk ślizgowych.* Oficyna Wydawnicza Politechniki Rzeszowskiej. Rzeszów, Poland 2019. [In Polish: *Lubrication theory of slidings bearings.* The Publishing House Rzeszow University of Technology].
31. DIN 51519 Lubricants - *ISO viscosity classification for industrial liquid lubricants*. Deutsches Institut für Normung. [In German: German Institute for standardization].
32. DIN 31652, Teil 1, 2, 3. *Hydrodynamische Radial – Gleitlagerimstationärem Betrieb*. Deutsches Institut für Normung. [In German: Plain bearings - *Hydrodynamic plain journal bearings under steady-state conditions*. German Institute for standardization].
33. Kaniewski, W. Warunki brzegowe diatermicznego filmu smarnego. *Zeszyty naukowe Politechniki Łódzkiej*. 1997. No. 14. P. 1-10. [In Polish: Boundary conditions of a diathermic lubricating film. *Scientific Journals of the Lodz University of Technology*].

Received 01.06.2021; accepted in revised form 15.09.2022